Antibacterial potential of silver nanoparticles synthesized using tri-sodium citrate via controlled exploitation of temperature

Y. Zaman[a], M. Z. Ishaque[a], R. Sattar[b], M. M. Rehman[b], I. Saba[c], S. Kanwal[a], M. Akram[a], M. Shahzad[a], H. Kanwal[d, e], R. Qadir[b], A. B. Siddique[e,*]
[a]*Department of Physics, University of Sargodha, Sargodha,40100, Pakistan*
[b]*Department of Chemistry, The university of Lahore, Sargodha Campus, Sargodha, 40100, Pakistan*
[c]*Department of Chemistry, GC Women University Sialkot, 51030, Pakistan*
[d]*Applied Chemistry Research Center, Pakistan Council of Scientific and Indusrial Research (PCSIR) Laboratories Complex, Lahore, 54600, Pakistan*
[e]*Institute of Chemistry, University of Sargodha, Sargodha, 40100, Pakistan*

In present work, synthesis of silver nanoparticles (AgNPs) has been reported by utilizing tri-sodium citrate (TSC) as reducing and stabilizing agent. The effect of temperature and molar ratio of silver salt ($AgNO_3$) and TSC has been studied on the size and morphology of nanoparticles. The synthesized AgNPs were characterized by Powder X-ray Diffraction (XRD), UV-Visible spectroscopy (UV-Vis.), Scanning Electron Microscopy (SEM) and Energy Dispersive X-ray spectroscopy (EDS). Biological evaluation of the optimized AgNPs against strains of gram-positive and gram-negative bacteria showed low to moderate values of inhibition zones as compared to standard rifampicin.

(Received March 19, 2022; Accepted September 1, 2022)

Keywords: Silver nanoparticles, Wet chemical route, Microstructural and morphological analysis, Optical properties

1. Introduction

Amongst the metal nanostructures, silver nanoparticles (AgNPs) have gained prime importance in numerous fields such as the optics, electronics, chemical analysis, solar energy, catalysis, biomedicine, and environment [1-2].

Owing to diverse applications, a low cost and robust method with good yields for the synthesis of AgNPs is a topic of interest for scientists. AgNPs synthesis with controlled morphology has been studied extensively in many diverse systems in last two decades [3]. AgNPs can be synthesized by biological methods [4], physical methods [5], and chemical reduction method [6]. Every method carried its own advantages and disadvantages such as physical method takes too much time for synthesis of AgNPs while biological method is eco-friendly, but it is very painful task. Chemical reduction method is advantagecious owing to its robustness, less time consumption with high yield but unfortunately it is not eco-friendly. However, its significance cannot be ignored over a single disadvantage [7-8]. Therefore, chemical reduction method is mostly used to synthesize AgNPs of desired size and morphology [9,10]. This method consists of two main steps: Reduction by using reducing agent like sodium borohydrate [11] followed by stabalization e.g. by citrate [12] and Polyvinylpyrrolidone (pvp) [13]. In chemical reduction method, organic and inorganic reducing agents are reported to reduce the salt of the main precursor. The selection of reducing agent is very important, because morphology and the size distribution of nanoparticles is highly dependent on it i.e. sodium boroydrate is used to synthesize small size NPs and citrate is used to synthesize relatively large sized NPs [14]. The morphology of nanoparticles can also be changed just by varying the molar ratio of main precursor and reducing agents [15], temperature [16], injection rate [17], reaction time [18] and pH of solution [19]. Tri-

* Corresponding author: abubakar.siddique@uos.edu.pk
https://doi.org/10.15251/DJNB.2022.173.979

sodium citrate (TSC) is a commonly used reducing agent to synthesize AgNPs by utilizing small amount of silver salt [20]. Basic chemistry behind the use of TSC is its dual function to work as reducing as well as stabilizing agent [21].

Temperature play an important role in size determination of AgNPs by changing the kinetics of aggregation of atoms. With the increase of temperature, reduction rate and aggregation of particles increases which results in increased size of AgNPs [22].

Many metal NPs are being biologically investigated for their antibacterial potential either in pure form or after coating of drugs. Among this class, AgNPs have gained prime importance due to their interaction with cell membrane of bacteria and binding ability with various proteins and enzymes containing sulphur and phosphorous atoms [23]. It has been currently investigated that these particles change the permeability of cell membrane of bacteria which leads to the leakage of cell material and ultimately death. Moreover, it has also been hypothesized that the AgNPs interact with the DNA and proteins of cell if they cross the porous cell membrane, ultimately inhibition of bacterial growth and death [24]. Due to antibacterial properties, AgNPs are being currently used in creams and ointments, used to cure for burn and wounds, to inhibit the growth of bacteria [25].

In current research work, AgNPs has been synthesized by wet chemical reduction method. Main precursors were silver nitrate ($AgNO_3$) as silver salt and Tri-sodium citrate ($C_6H_5Na_3O_7.2H_2O$) as a reducing agent. The effect of molar ratio of $AgNO_3$ and TSC by keeping temperature constant and by varying reaction temperature were analysed on the size and shape of AgNPs. Antibacterial potential of the synthesized AgNPs was evaluated against gram-positive and gram-negative bacterial strains.

2. Experimental

2.1. Synthesis of silver nanoparticles

For the preparation of AgNPs, $AgNO_3$ 0.17, 0.34 and 0.68 g was dissolved in 100 mL of distilled water. The solutions were heated along with the stirring till the temperature was stabilized at 80 ^oC. TDS solution (0.1, 0.2 and 0.4 M) was added drop wise in the vigorously stirred fractions of $AgNO_3$ solutions. The fractions were kept on stirring for one hour. Each fraction was centrifuged at 10,000 rpm to separate AgNPs and then cooled at room temperature. Finally, the collected AgNPs were dried at 45 ^oC in oven. Similarly, three samples of AgNPs were synthesized at temperature 60, 80 and 90 ^oC by keeping constant molar ratio (0.02/0.2) of $AgNO_3$ and TSC.

2.2. Antibacterial activity of AgNPs

Disc diffusion method was used to determine the antibacterial activity of AgNPs. Four bacterial strains, two gram-positive (*S. aureus, B. subtilis*) and two gram-negative (*E. coli, P. multocida*) were used to evaluate the antibacterial potential of NPs. Bacterial strains were maintained in nutrient agar (20 g/L) for 24 h at 4 □C. The turbidity of the nutrient broth of each starin was adjusted by addition of saline (0.9% NaCl). This broth was used for seedling the nutrient agar which was prepared by mixung of 2 g of agar in 100 mL of distilled water. This agar medium was autoclaved and cooled down to 40 □C after maintaining the pH of 7.0. This agar medium was seeded with 1 mL of inoculum. Then, 25 mL of seeded agar medium was placed in petri dish and allowed to solidify. Sterile paper disc loaded with AgNPs in DMSO were placed in petri dish of each strain. DMSO was used as negative control and standard broad spectrum antibiotic drug Rifampicin (1 mg/mL) was used as positive control. Petri dishes were incubated for 24 h at 37 □C. The zone of inhibition of AgNPs was measured in each strain by comparing with standard drug.

3. Results and discussions

3.1. X-Ray diffraction analysis

XRD patterns of AgNPs, which were prepared by varing molar ratio of $AgNO_3$ and TSC at

constant temperature, are shown in Fig.1. Four diffraction peaks were observed for each sample at 28.0°, 31.9°, 38.0°, and 44.1°, which corresponded to (100), (110), (111) and (200) reflections. All these reflections confirmed the FCC structure of AgNPs. The most intensive peak for FCC structure was found at (100) [26]. So, the synthesis of AgNPs and their crystallinity were confirmed (by JCPDS file no.00-076-1393). It was observed that broadening of diffracted peaks were decreased as the crystallite size was decreased by increasing the molar ratio of $AgNO_3$ and TSC. For the 0.01/0.1, 0.02/0.2 and 0.04/0.4 molar ratios of $AgNO_3$ and TSC at 80 °C, the crystallite sizes were found 32, 29 and 25 nm, respectively.

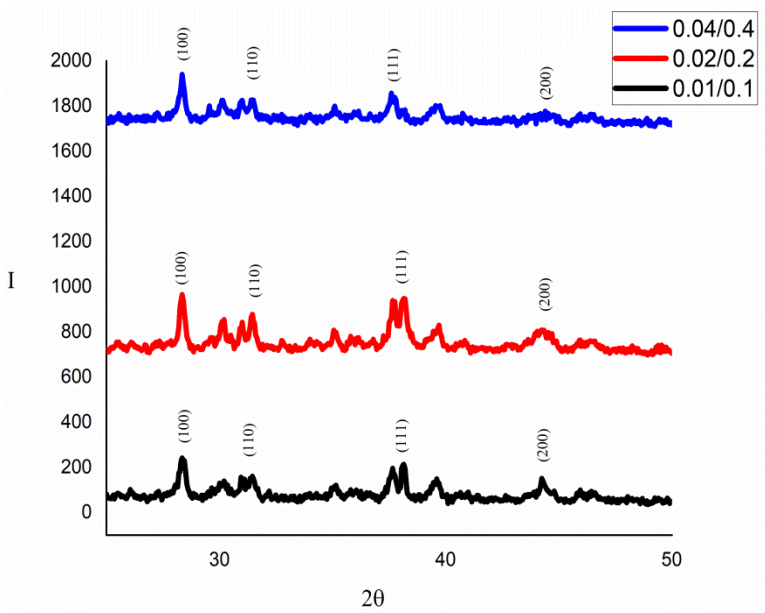

Fig. 1. XRD pattern of AgNPs prepared using different concentration ratios of $AgNO_3$/TSC (0.01/0.1, 0.02/0.2 and 0.04/0.4) at 80 °C temperature.

For 60 and 80 °C, the strong number of Bragg's reflections was seen at 2Θ values of 28.0°, 31.9°, 38.0°, and 44.1°, which corresponded to the (100), (110), (111) and (200) reflections and for 95 °C, strong number of Bragg's reflections was seen at 38.1°, 44.2°, 64.4° and 77.3°, which corresponded to the (111), (200), (220) and (311) reflections as shown in Fig.2. All these reflections confirmed the FCC structure of AgNPs. The most intensive peak for FCC structure is (100). So, synthesis of AgNPs and their crystallinity was confirmed (by JCPDS file no. 00-076-1393). The most intensive peak for FCC structure was found at (100) and (111) [27]. It was observed that the size of AgNPs was increased continuously with increase of temperature due to fast aggregation of atoms [28]. For the constant molar ratio (0.02/0.2) at 60, 80 and 95 °C, crystallite size was found 25, 29 and 30 nm, respectively.

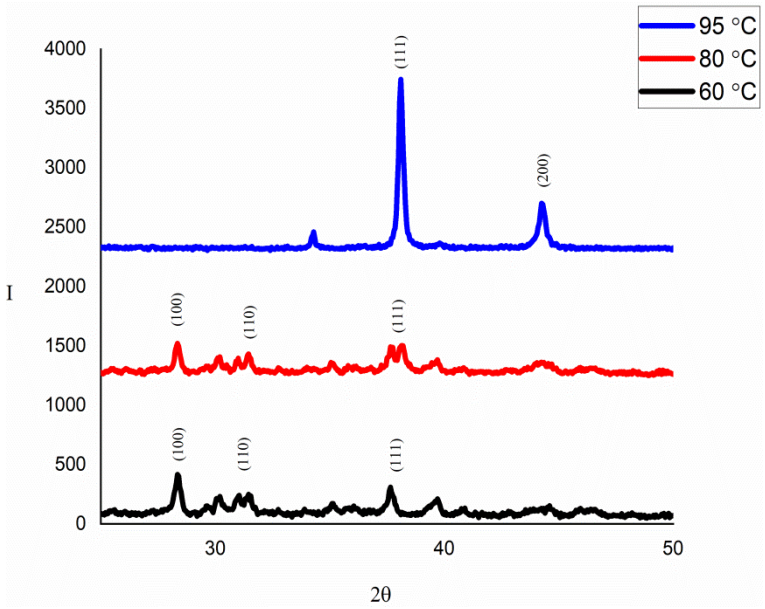

Fig. 2. XRD patterns of AgNPs prepared by different temperature 60, 80 and 95 °C at constant concentration ratio (0.02/0.2) of $AgNO_3$/TSC.

3.2. UV-Visible spectra

By variation of molar ratio of $AgNO_3$ and TSC at contant temperature (80 °C), blue shift of peaks was observed as shown in Fig.3. It was seen that, the size of AgNPs decreased with increasing the concentrations of $AgNO_3$ and TDS. Absorption maxima were found at 459, 440 and 378 nm for the molar ratio of 0.01/0.1, 0.02/0.2, 0.04/0.4. Moreover, this effect was also confirmed by previously reported literature [29].

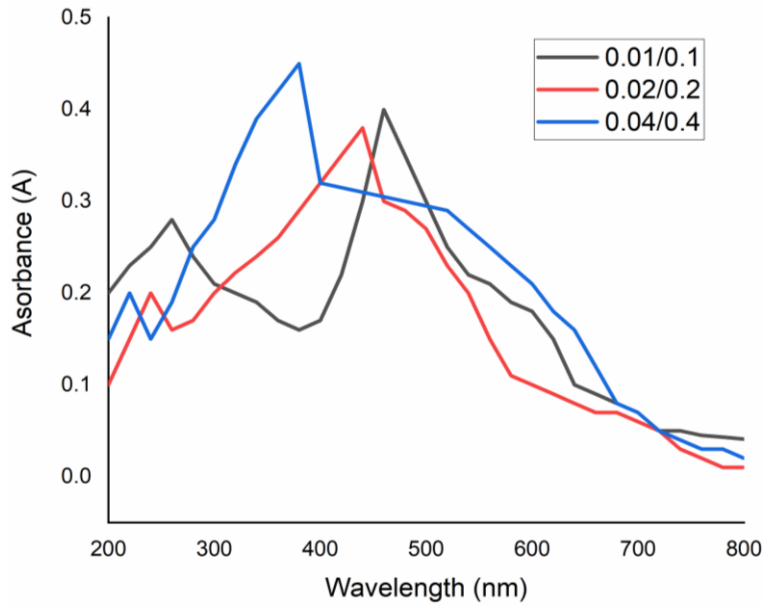

Fig. 3. UV-visible spectra of $AgNO_3$/TSC at 80 °C temperature for different molar ratios of $AgNO_3$ and TDS: (a) 0.01/0.1 (b) 0.02/0.2 (c) 0.04/0.4.

Effect of temperature on the size of AgNPs was studied by keeping the molar ratio of $AgNO_3$ and TSC constant (0.02/0.2). With the increase of temperature, the size of AgNPs was

increased which was confirmed by red shift of absortion maxima peaks as shown in Fig. 4. Absorption maxima was shifted from 389 to 440 and 445 nm at temperature of 80 and 95 ^{o}C, respectively. This increase in size of NPs was attributed to the fast aggregation of particles at high temperature [30].

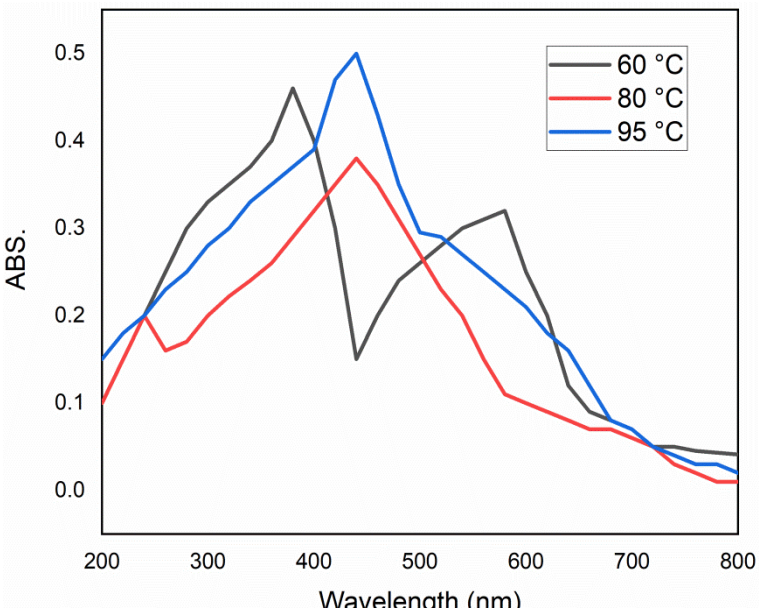

Fig. 4. UV-visible spectra of 0.02/0.2 concentration of $AgNO_3$/TSC at: (a) 60 ^{o}C temperature (b) 80 ^{o}C temperature (c) 95 ^{o}C temperature.

3.3. Energy dispersive X-ray spectroscopy (EDS)

Purity of the synthesized AgNPs was confirmed by EDS (Fig. 5) which was found 98.62% by weight and 88.84% by atom with impurity of carbon 1.38% by weight and 11.16% by atom as shown in Table 1.

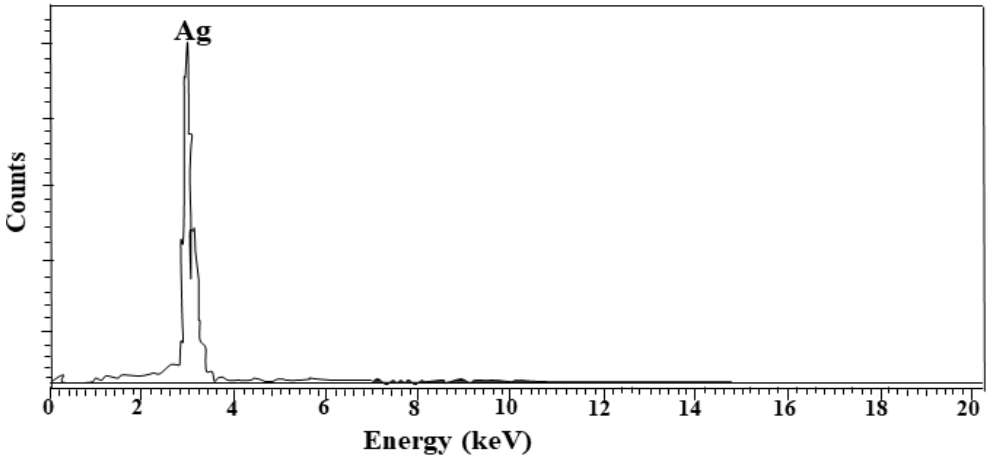

Fig. 5. EDS compositional intensity of AgNPs ($AgNO_3$).

Table 1. Compositional weight percentage of EDS.

Element	Weight%	Atomic%
C K	1.38	11.16
Ag L	98.62	88.84
Totals	100.00	

3.4. Scanning Electron Microscopy (SEM)

SEM images of the synthesized AgNPs were taken to determine the morphology and size. At 80 ^{o}C, size of AgNPs for concentration ratios of 0.01/0.1, 0.02/0.2 and 0.04/0.4 was found 332, 196 and 178 nm, repectively as shown in the Fig. 6, Fig. 7 and Fig. 8, respectively. All the particles aggregated to form flakes at this temperature.

By keeping the molar ratio of $AgNO_3$ and TSC constant (0.02/0.2), the effect of temperature was studied on size and morphology of particles as shown in Fig. 7, Fig. 9 and Fig. 10. It was seen that the size of particles goes on decreasing with the increase of temperature. The AgNPs prepared at 60, 80 and 95 ^{o}C were found in the form of distinct flakes, nanorods and nano spheres having average size 290, 196 and 121 nm, respectively.

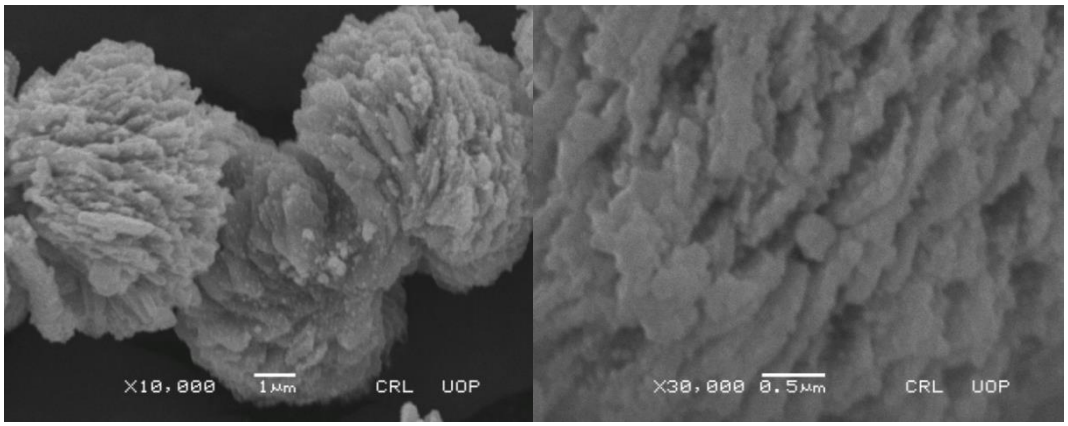

Fig. 6. SEM image of AgNPs at molar ratio (0.01/0.1) of $AgNO_3$ and TSC at 80 ^{o}C.

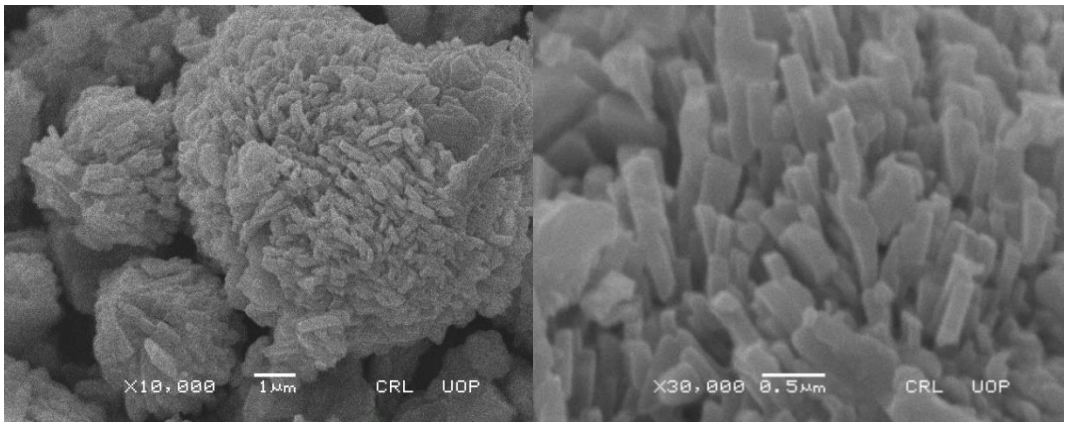

Fig. 7. SEM image of AgNPs at molar ratio (0.02/0.2) of $AgNO_3$ and TSC at 80 ^{o}C.

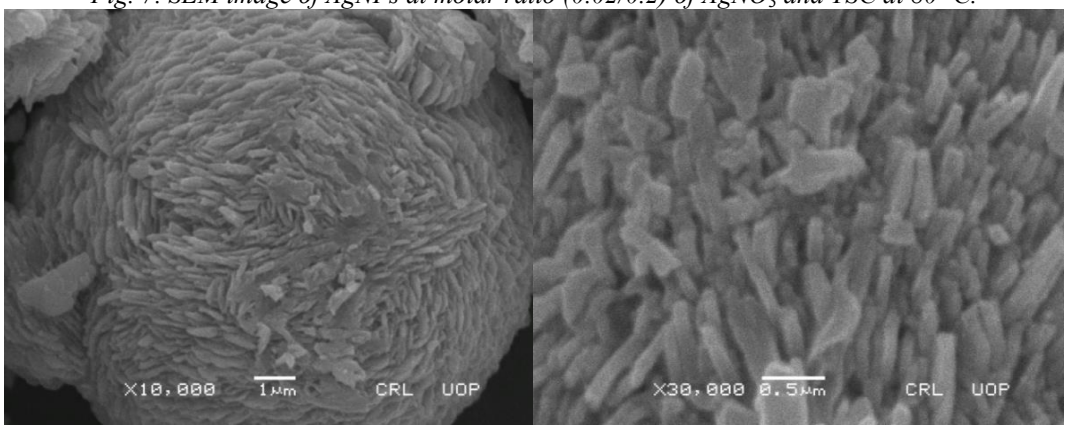

Fig. 8. SEM image of AgNPs at molar ratio (0.04/0.4) of $AgNO_3$ and TSC at 80 ^{o}C

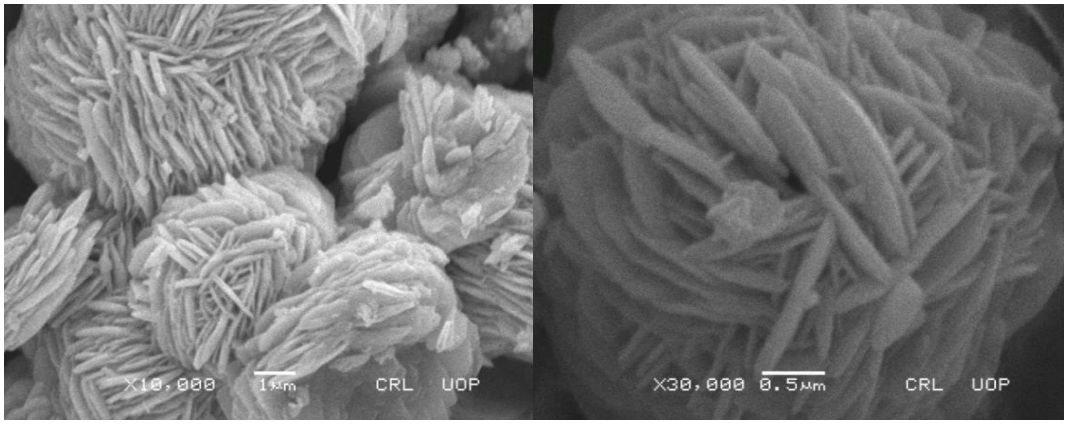

Fig. 9. SEM image of AgNPs at molar ratio (0.02/0.2) of $AgNO_3$ and TSC at 60 ^oC.

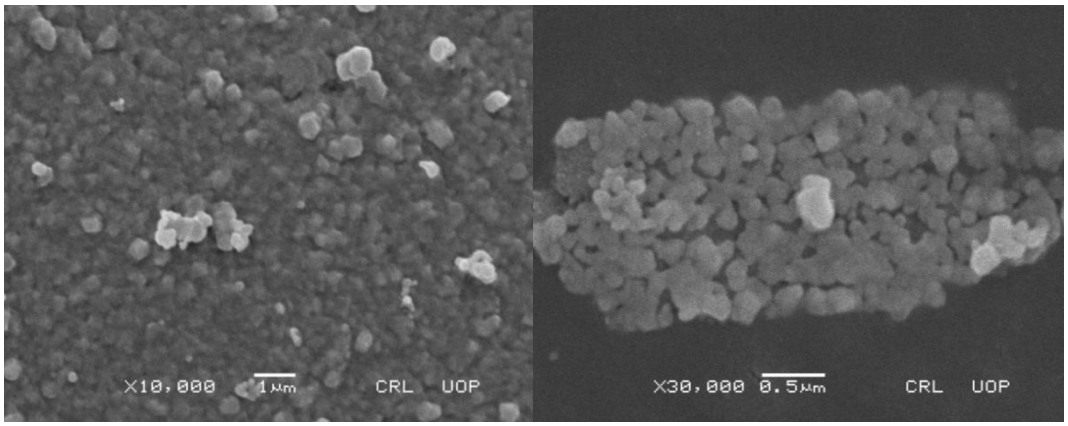

Fig. 10. SEM image of AgNPs at molar ratio (0.02/0.2) of $AgNO_3$ and TSC at 95 ^oC.

3.5. Antibacterial activity

The antibacterial activity of AgNPs synthesized at optimum conditions (0.02/0.2 at *95 ^oC*) showed they were more active against the gram-negative bacteria. The inhibition zone against gram-negative strains *Escherichia coli* and *Pasturella multosida* were 15 ± 0.2 and 13 ± 0.1 mm, respectively as compared to the gram-positive strains i.e., *Staphylococcus aureus and Bacillus subtilis* with inhibition zone of 9 ± 0.3 and 8 ± 0.2 mm, respectively. More activity against the gram-negative bacteria was attributed to the different structure of cell wall of this strain. Cell wall of gram-negative bacteria is relatively thin which result in the more penetration of AgNPs in the cell, as reported in literature [31].

Table 2. Inhibition zones of bacterial growth.

	Zone of inhibition (mm)			
	Gram-Negative Bacteria		***Gram-Positive Bacteria***	
Sample	***E. coli***	***P. multocida***	***S. aureus***	***B. subtilis***
AgNPs	15 ± 0.2	13 ± 0.1	9 ± 0.3	8 ± 0.2
Rifampicin (Standard)	28 ± 0.2	25 ± 0.01	21 ± 0.2	18 ± 0.3

4. Conclusion

In the present work, the synthesis of AgNPs has been reported under controlled parameters i.e., temperature and molar ratio, through a chemical reduction method. XRD analysis confirmed the pure phase FCC crystal structure of the AgNPs. The reaction temperature and the molar ratio of main precursor and reducing agent were very influential at the morphology of AgNPs. UV-visible absorption peaks from 378 to 450 nm confirmed the synthesis of AgNPs. Increase in both main precursor and reducing agent concentrations led to the blue shift in absorption bands and increase in temperature led to red shift which depicted the size variation of AgNPs. SEM confirmed the different morphology and size of AgNPs. The antibacterial potential of the AgNPs evaluated against different strains of bacteria showed that the AgNPs can be employed as an alternate to traditional drugs for the inhibition of the bacterial infections at moderate level. Moreover, the AgNPs can be further evaluated for their effectiveness against drug resistant gram-negative bacterial strains.

Acknowledgements

This work was financially supported by Higher Education Commission Start up research grant Program No: 21-2079/SRGP/R&D/HEC/2018.

References

[1] A. R. Tao, S. Habas, P. Yang, Shape, Small 4(3), 310 (2008); https://doi.org/10.1002/smll.200701295

[2] B. Domènech, J. Bastos-Arrieta, A. Alonso, J. Macanás, M. Munoz, D. N. Muraviev, "Ion exchange technologies", IntechOpen, Croatia, 35 (2012).

[3] S. E. Skrabalak, L. Au, X. Li, Y. Xia, Nature protocols 2(9), 2182 (2007); https://doi.org/10.1038/nprot.2007.326

[4] A. M. Fayaz, K. Balaji, M. Girilal, R. Yadav, P. T. Kalaichelvan, R. Venketesan. Nanotechnology, Biology and Medicine 6(1), 103 (2010); https://doi.org/10.1016/j.nano.2009.04.006

[5] T. Tsuji, K. Iryo, N. Watanabe, M. Tsuji, Applied surface science 202(2), 80 (2002); https://doi.org/10.1016/S0169-4332(02)00936-4

[6] A. Khan, A. Rashid, R. Younas, R. Chong, International Nano Letters 6(1), 21 (2016); https://doi.org/10.1007/s40089-015-0163-6

[7] E. M. Modan, A. G. Plaiaşu, Metallurgy and Materials Science 43(1), 53 (2020); https://doi.org/10.35219/mms.2020.1.08

[8] G. Sathiyanarayanan, G. S. Kiran, J. Selvin, Colloids and Surfaces B: Biointerfaces, 102, 13 (2013); https://doi.org/10.1016/j.colsurfb.2012.07.032

[9] Y. Yang, S. Matsubara, L. Xiong, T. Hayakawa, M. Nogami, The Journal of Physical Chemistry C 111(26), 9095 (2007); https://doi.org/10.1021/jp068859b

[10] S. H. Im, Y. T. Lee, B. Wiley, Y. Xia, Angewandte Chemie 44(14), 2154 (2005); https://doi.org/10.1002/anie.200462208

[11] K. Li, X. Jia, A. Tang, X. Zhu, H. Meng, Y. Wang, Integrated Ferroelectrics 136(1), 9 (2012); https://doi.org/10.1080/10584587.2012.686405

[12] M.G. Guzmán, J. Dille, S. Godet, Int J Chem Biomol Eng 2(3), 104 (2009).

[13] K. Ranoszek-Soliwoda, E. Tomaszewska, E. Socha, P. Krzyczmonik, A. Ignaczak, P. Orlowski, J. Grobelny, Journal of Nanoparticle Research 19(8), 1 (2017); https://doi.org/10.1007/s11051-017-3973-9

[14] A. Pyatenko, M. Yamaguchi, M. Suzuki, The Journal of Physical Chemistry C 111(22), 7910 (2007); https://doi.org/10.1021/jp071080x

[15] Y. Sun, Y. Xia, Science 298(5601), 2176(2002); https://doi.org/10.1126/science.1077229
[16] A. Nanda, M. Saravanan, Nanomedicine: Nanotechnology, Biology and Medicine, 5(4), 452 (2009); https://doi.org/10.1016/j.nano.2009.01.012
[17] D. Kim, S. Jeong, J. Moon, Nanotechnology 17(16), 4019 (2006); https://doi.org/10.1088/0957-4484/17/16/004
[18] S. Yazdani, A. Daneshkhah, A. Diwate, H. Patel J. Smith, O. Reul, A.R. Hajrasouliha, ACS omega 6(26), 16847 (2021); https://doi.org/10.1021/acsomega.1c01418
[19] L. Marciniak, M. Nowak, A. Trojanowska, B. Tylkowski, R. Jastrzab, Materials 13(23), 5444 (2020); https://doi.org/10.3390/ma13235444
[20] R. La Spina, D. Mehn, F. Fumagalli, M. Holland, F. Reniero, F. Rossi, D. Gilliland, Nanomaterials 10(10), 2031 (2020); https://doi.org/10.3390/nano10102031
[21] C. Karthik, K. V. Radha, Digest Journal of Nanomaterial and Biostructure, 7(3), 1007 (2012).
[22] N. Samadi, D. Golkaran, A. Eslamifar, H. Jamalifar, M. R. Fazeli, F. A. Mohseni, Journal of Biomedical Nanotechnology, 5(3), 247 (2009); https://doi.org/10.1166/jbn.2009.1029
[23] K. S. Siddiqi, A. Husen, R. A. K. Rao, Journal of nanobiotechnology 16(1), 1 (2018); https://doi.org/10.1186/s12951-018-0334-5
[24] C. Liao, Y. Li, S.C Tjong, International journal of molecular sciences 20(2), 449(2019); https://doi.org/10.3390/ijms20020449
[25] P. Khandel, S.K. Shahi, D. K. Soni, R. K., Yadaw, L. Kanwar, Nano convergence 5(1), 1 (2018); https://doi.org/10.1186/s40580-018-0167-9
[26] P. Pourali, M. Baserisalehi, S. Afsharnezhad, J. Behravan, H. Alavi, B. B. A. Hosseini, Journal of Pure and Applied Microbiology, 6(2), 757 (2012).
[27] D. P. Tamboli, D. S. Lee, Journal of hazardous materials, 260, 878 (2013); https://doi.org/10.1016/j.jhazmat.2013.06.003
[28] S. Ravichandran, V. Paluri, G. Kumar, K. Loganathan, B.R. Kokati Venkata, Journal of Experimental Nanoscience 11(6), 445 (2016); https://doi.org/10.1080/17458080.2015.1077534
[29] N. Senthilkumar, S.S. Raadha, S. Udayavani, International Journal of Production Engineering 1(1), 25 (2015).
[30] S. V. Otari, R. M. patel, N. H. Nadaf, S. J. Ghosh, S. H. Pawar, Environmental Science and Pollution Research 21(2), 1503 (2014); https://doi.org/10.1007/s11356-013-1764-0
[31] T.G. Meikle, B.P. Dyett, J.B. Strachan, J. White, C.J. Drummond, C.E. Conn, ACS Applied Materials & Interfaces 12(6), 6944 (2020); https://doi.org/10.1021/acsami.9b21783